

Improvement of the Mechanical Properties of an Ultrahigh Molecular Weight Polyethylene Fiber/Epoxy Composite by Corona-Discharge Treatment

TOSHIO OGAWA, HIROAKI MUKAI, SATOSHI OSAWA

Laboratory for Ecological Polymer and Organic Materials, Kanazawa Institute of Technology, 7-1, Ohgigaoka, Nonoichi, Ishikawa, 921-8501 Japan

Received 10 November 1999; accepted 7 April 2000

ABSTRACT: The interfacial shear strength of an ultrahigh molecular weight (UHMW) polyethylene (PE) fiber/epoxy-resin system was greatly improved by the corona-discharge treatment of the fiber. The UHMW PE-fiber/epoxy-resin composite was prepared with corona-discharge-treated UHMW PE fiber. The mechanical properties of the composite sheet were determined by tensile testing. The tensile strength of the composite was also very much improved. However, the tensile strength of the composite was about one-half of the theoretical strength. This result was due to the molecular degradation of the PE-fiber surface caused by surface modification. © 2000 John Wiley & Sons, Inc. *J Appl Polym Sci* 79: 1162–1168, 2001

Key words: ultrahigh molecular weight; polyethylene fiber; interfacial shear strength; corona-discharge treatment; composite

INTRODUCTION

High-performance fibers, such as carbon, aramid, and polyethylene (PE), have been developed and applied to various fields. High-strength PE fiber was developed via a gel spinning method in the 1980s.¹ This highly oriented or drawn fiber² has an extremely high tensile strength and elastic modulus, 2.83 and 100 GPa, respectively, and has been applied in various ways, such as rope for use at sea.^{3,4}

High-performance polymer sheets have been developed to satisfy various industrial fields.⁵ If we can prepare a composite of an ultrahigh molecular weight (UHMW) PE fiber with some ma-

trix, the composite is expected to have high performance and lightness. Fiber/low-density PE and fiber/high-density PE composites were prepared by compression molding.⁶ In this study, epoxy resin was chosen because this resin is excellent in its interfacial properties with fiber and has been applied by industries in various fields. However, PE fiber is nonpolar on its surface and is expected to have very weak compatibility with other resins unless there is some treatment. There are many methods to modify the polymer surface.⁷ In this study, corona-discharge treatment^{8–10} was conducted for the PE fiber. This treatment is simpler and more practical than any other chemical^{11–13} and physical^{14–21} methods because samples are treated in air under atmospheric pressure. In this article, the mechanism of interfacial failure is discussed with respect to PE/epoxy composites on the basis of the results of X-ray photoelectron spectroscopy (XPS) analysis.

Correspondence to: T. Ogawa (E-mail: tsogawa@neptune.kanazawa-it.ac.jp)

Journal of Applied Polymer Science, Vol. 79, 1162–1168 (2001)
© 2000 John Wiley & Sons, Inc.

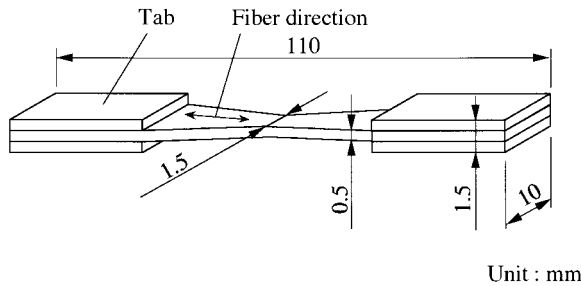


Figure 1 Schematic illustration of a tensile test specimen.

EXPERIMENTAL

Materials

Tekmilon fiber (Mitsui Chemical Industries, Ltd., Tokyo, Japan) was used as the UHMW PE fiber. The fiber was used for our experiments after being washed with benzene, ethanol, and water. The existence of oxygen (7.3 atom %) was confirmed on the surface by XPS after this washing. Therefore, it was estimated that some surface treatment had already been carried out. The epoxy resin and hardener used were Epikoto 828 and Epomate LX-1N (Yuka Shell Epoxy, K.K., Tokyo, Japan), respectively. These compounds were used in a 70/30 wt % ratio (Epikoto/Epomate). Some of the properties of these materials are described in detail in a previous article.²²

Corona Treatment

The corona-discharge treatment was performed with an HPS-10, a commercial machine made by Nippon Static Co., Ltd. (Tokyo, Japan). The performance of the machine was as follows: a maximum discharge voltage of 15 kV and a discharge frequency of 20 kHz.²²

Surface Analysis

The spectra of the PE fiber were obtained with an ESCA-850 XPS (Shimadzu Co., Ltd., Kyoto, Japan). The C_{1s} peak was separated into several peaks due to functional groups with a curve resolver installed in the instrument.

Macroscopic Properties

The tensile strength and elastic modulus of the composite were determined with an AGS-1000B tensile tester (Shimadzu) at a velocity of 2 mm/

min. We prepared the specimen as a unidirectional fiber-reinforced composite with the PE fiber and epoxy resin containing the hardener by keeping it at 80 °C for 3 h. The determined volume fraction of the PE fiber in the composite was 0.40. This value was obtained from a microphotograph of a cross section of the composite. The shape of the specimen for the tensile test is shown in Figure 1. The tensile test for the fiber and epoxy sheet was performed according to JIS L 1069 at a test speed of 20 mm/min and according to JIS K 7113 in type I at a test speed of 10 mm/min.

Microscopic Properties

The interfacial shear strength (IFSS) was determined by the microbond pull-out method, which is described in detail elsewhere.²² A droplet of epoxy resin containing the hardener was deposited onto the fiber surface and cured at 80 °C for 3 h.

The shearing test specimen of the composite was prepared with PE-fiber sheet and epoxy resin containing the hardener at 80 °C for 3 h. The PE-fiber sheet was molded from only PE fibers. The melting point and heat of fusion of the PE-fiber sheet were 2 °C and 40 mJ/mg, respectively, less than the values of the original PE fiber.⁶ The PE-fiber sheet was prepared in $6 \times 2 \times 20$ mm and was adhered to the epoxy resin on 6×6 mm into a $6 \times 2 \times 20$ mm mold, as shown in Figure 2. The shearing test was carried out with a tensile tester at a test speed of 0.5 mm/min.

RESULTS AND DISCUSSION

The corona-discharge treatment for the fiber was performed only once in a previous study.²² In this treatment, the upper side of the fiber was mainly

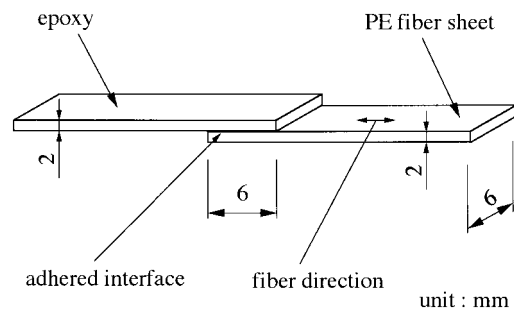


Figure 2 Schematic illustration of a shear test specimen.

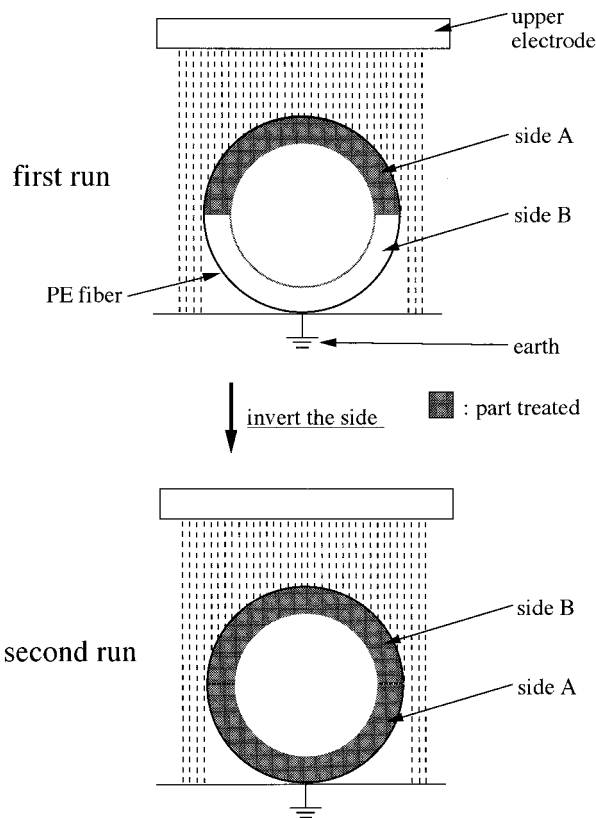


Figure 3 Schematic diagram of the first-running and second-running corona-treatment method.

treated because the cross section of the fiber was round. However, the lower side was not treated sufficiently, as shown in Figure 3. Table I shows the oxygen content on the surface of the PE fiber from the XPS analysis. The oxygen content of the

Table I Oxygen Contents of the PE-Fiber Surface

	Side	Oxygen Content (atom %)
Untreated	—	7.3
First running ^a	A	20.2
First running ^b	A	23.5
First running ^a	B	18.3
First running ^b	B	20.7
Second running ^a	A	27.1
Second running ^b	A	29.9
Second running ^a	B	27.4
Second running ^b	B	29.9

^a Treated in $3.6 \times 10^4 \text{ J/m}^2$ by corona discharge.

^b Treated in $4.4 \times 10^4 \text{ J/m}^2$ by corona discharge.

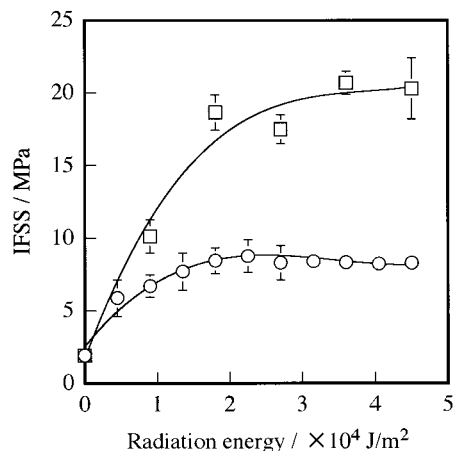


Figure 4 IFSS of the PE/epoxy composite as a function of the corona radiation energy: experimental values of the first running (○) and the second running (□).

untreated fiber was 7.3 atom % [O/(C + O)] because we used commercially available PE fiber. The A and B sides in the fiber are shown in Figure 3. The oxygen content of the B side was less than that of the A side in the first running. The electrons and ions were generated mainly between an upper electrode and the upper side of the fiber and rarely reacted with the surface in the B side. Then, the fiber was turned over after the first corona treatment and was treated again by corona discharge, i.e., the second running. The oxygen content of the B side treated by the second running became almost equal to that of the A side. The oxygen content of the A and B sides in

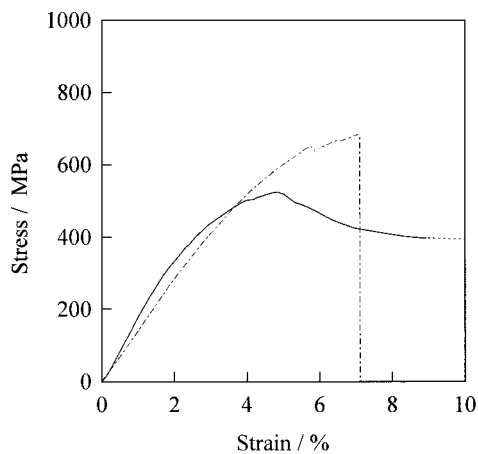
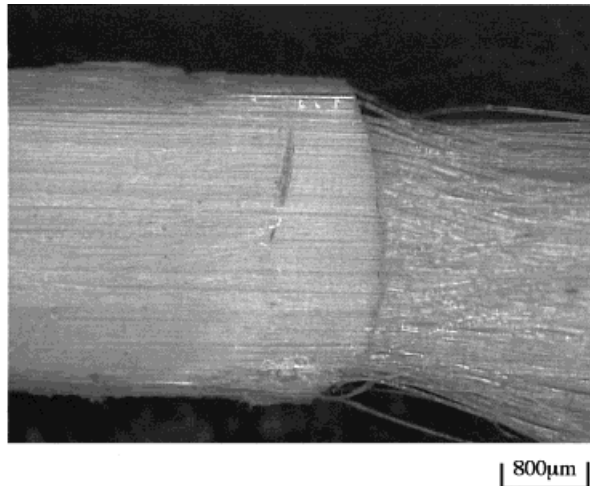
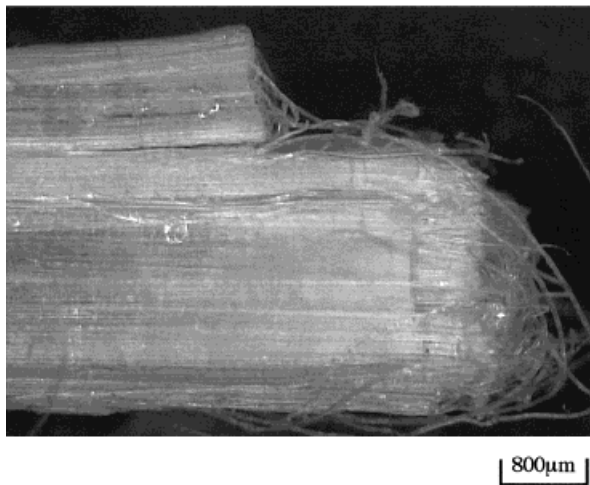


Figure 5 Typical stress–strain curves: the untreated fiber composite (—) and the second-running corona-treated ($3.8 \times 10^4 \text{ J/m}^2$) fiber composite (---).



(a)



(b)

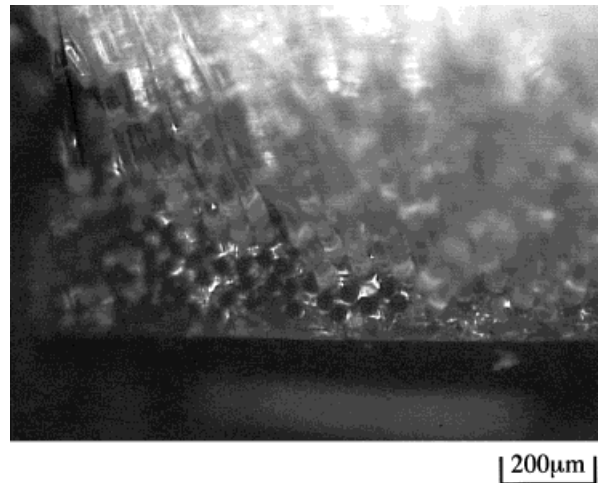
Figure 6 Charge-coupled device micrographs of fractures in a tensile test observed in the longitudinal direction to the fiber: (a) an untreated fiber composite and (b) a corona-treated ($3.8 \times 10^4 \text{ J/m}^2$) fiber composite.

the second running was 9.2 atom % larger than that of the B side in the first running. The oxygen content of the fiber surface in the first running was not homogeneous. The oxygen content in the second running became homogeneous, as shown in Table I.

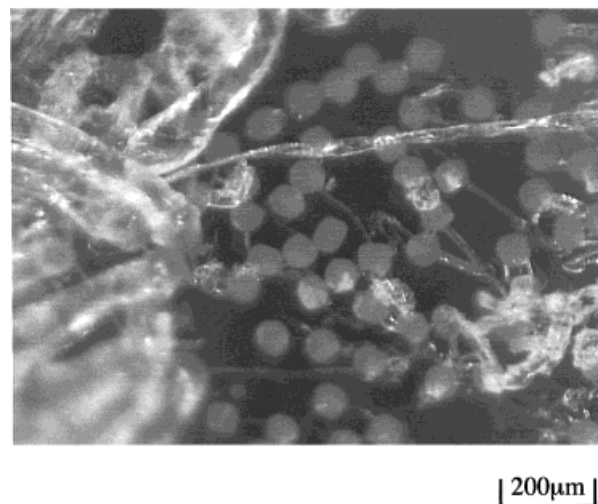
The IFSS between the PE fiber and the epoxy resin was determined by the microbond pull-out method. The IFSS is shown in Figure 4. The highest value was 8 MPa in the first running of the corona-discharge treatment. However, the IFSS

after the second-running treatment was about twice the IFSS of the first-running one. The IFSS maximum value was 20 MPa in the second-running treatment. This high value has not yet been reported elsewhere.

The mechanical properties of the composite were determined by tensile testing. Figure 5 shows typical stress-strain curves for the composite. The stress in the untreated fiber composite reached a maximum at 4–5% strain, but the composite was broken at a large strain. The stress in the corona-treated fiber composite reached a max-



(a)



(b)

Figure 7 Charge-coupled device micrographs of fractures in a tensile test observed in the cross-sectional direction: (a) an untreated fiber composite and (b) a corona-treated ($3.8 \times 10^4 \text{ J/m}^2$) fiber composite.

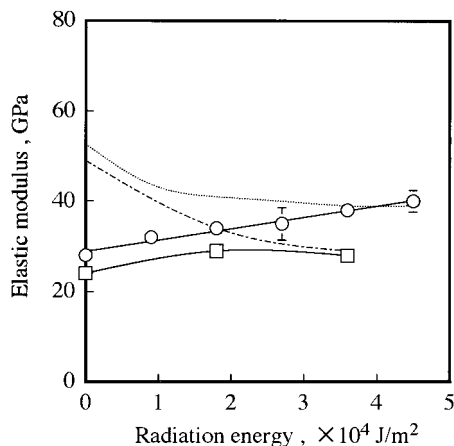


Figure 8 Elastic modulus of the PE/epoxy composite as a function of the corona radiation energy: experimental values of the first running (\circ), experimental values of the second running (\square), predicted theoretical curve for the first running (\cdots), and predicted theoretical curve for the second running ($- \cdot -$).

imum at 7–8%, and a catastrophic change was observed in the stress–strain curve. The adhesion of the untreated fiber with epoxy resin was not sufficient, as shown by black empty sockets in Figures 6(a) and 7(a). However, a typical failure pattern in the treated fiber composite is shown in Figures 6(b) and 7(b).

The elastic modulus of the composite is shown in Figure 8. The predicted theoretical values for the tensile strength (σ_c) and elastic modulus (E_c) of the composite were calculated with the linear mixture rule:²³

$$\sigma_c = \sigma_f^* V_f + \sigma'_m (1 - V_f) \quad (1)$$

$$E_c = E_f V_f + E_m (1 - V_f) \quad (2)$$

where σ_f^* and σ'_m are the tensile strength of the PE fiber and the resin at break, respectively. E_f and E_m are the elastic modulus of the PE fiber and the resin, respectively. The fiber and resin were treated independently under the same conditions as those for the composite, and σ_f^* , σ'_m , E_f , and E_m were determined with tensile testers. The elastic modulus of the fiber decreased in the second-running treatment compared with the elastic modulus for the first running. The experimental elastic modulus of the composite agreed with the predicted theoretical one in both cases with large radiation energy in the corona treatment. The

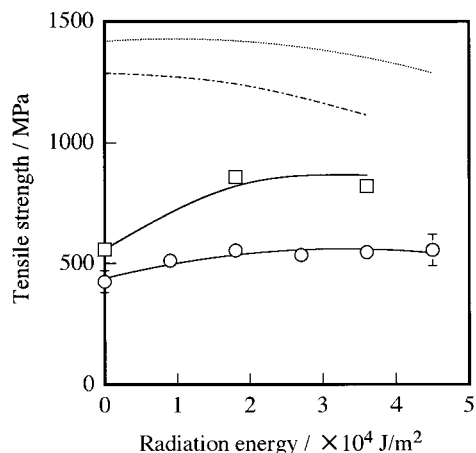


Figure 9 Tensile strength of the PE/epoxy composite as a function of the corona radiation energy: experimental values of the first running (\circ), experimental values of the second running (\square), predicted theoretical curve for the first running (\cdots), and predicted theoretical curve for the second running ($- \cdot -$).

results for the tensile strength are shown in Figure 9. The experimental value gave only 41% of the theoretical value at $3.7 \times 10^4 \text{ J/m}^2$ in the first running. The experimental value of the second-running treatment was improved to 70% of the theoretical value. However, this value was not sufficient in comparison with the values of carbon-fiber-reinforced plastics.²⁴

Thus, we tried to discover the reason the mechanical strengths of the composite were weak.

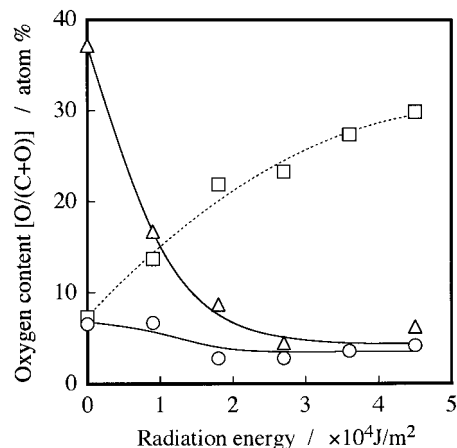


Figure 10 Oxygen content (atom %) as a function of the corona radiation energy: the PE-sheet surface before the shearing test (\square), the PE-sheet side after the shearing test (\circ), and the epoxy-resin side after the shearing test (\triangle).

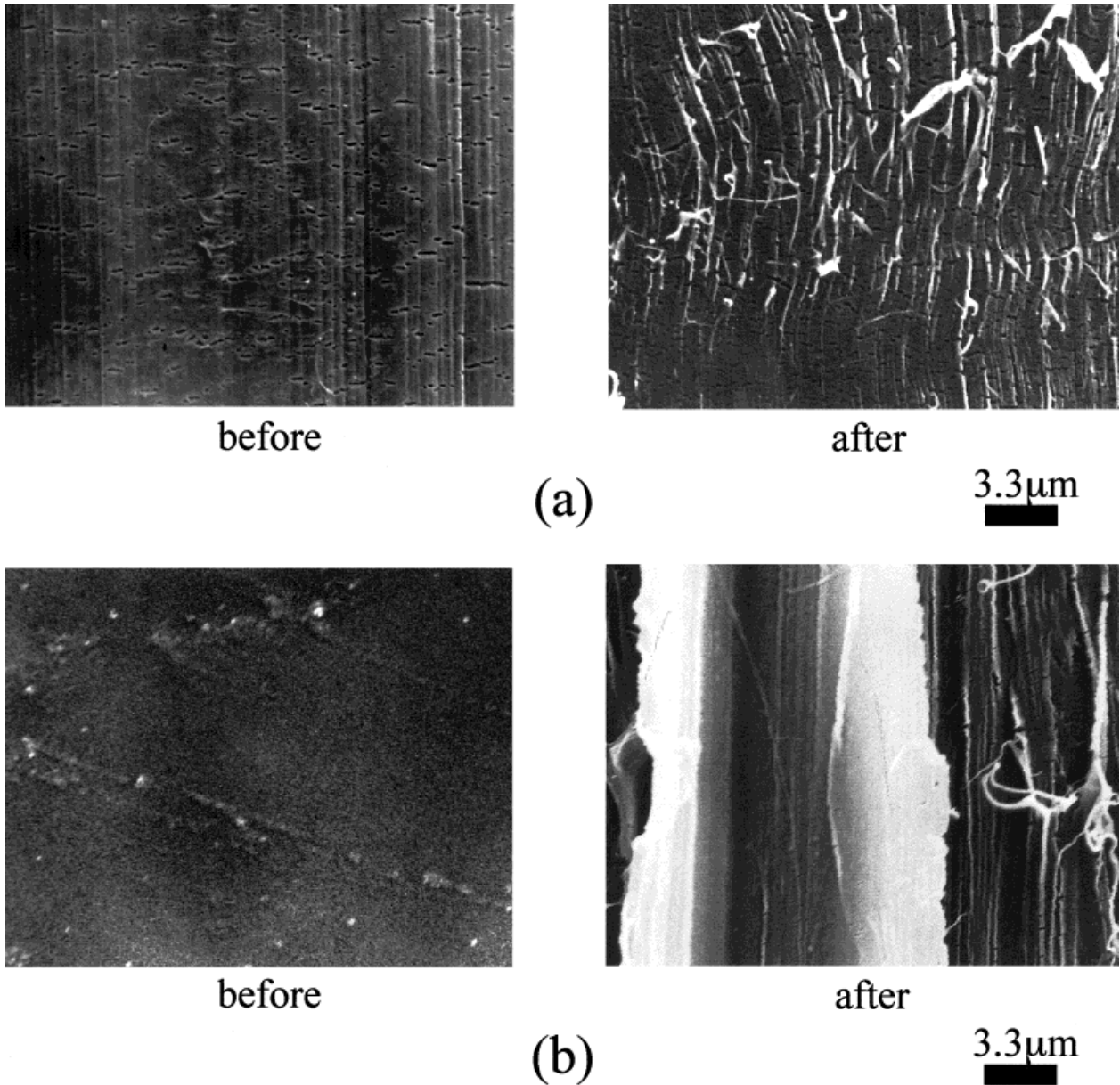


Figure 11 Scanning electron micrographs of the fractured surfaces in the shearing test: (a) the PE side and (b) the epoxy-resin side.

Namely, a shearing test was conducted for the tensile specimen prepared with PE fiber and epoxy-resin board, the details of which are given in the Experimental section. The oxygen contents of the fractured surfaces were determined by XPS. The result is shown in Figure 10. The oxygen content of the epoxy-resin side, about 37 atom % at zero radiation energy, is that of the epoxy resin itself. This value is completely in agreement with the calculated value. The oxygen content of the

PE side, 7.3 atom %, is that of the untreated PE fiber at zero radiation energy. After the shearing test, the oxygen contents in the epoxy-resin side decreased with the increase of the radiation energy. The oxygen content in the PE-fiber side decreased slightly with the increase of the radiation energy. With the high-radiation energy, the oxygen contents almost coincided with each other and reached about 4 atom %. This value was lower than that of the untreated fiber (7.3 atom

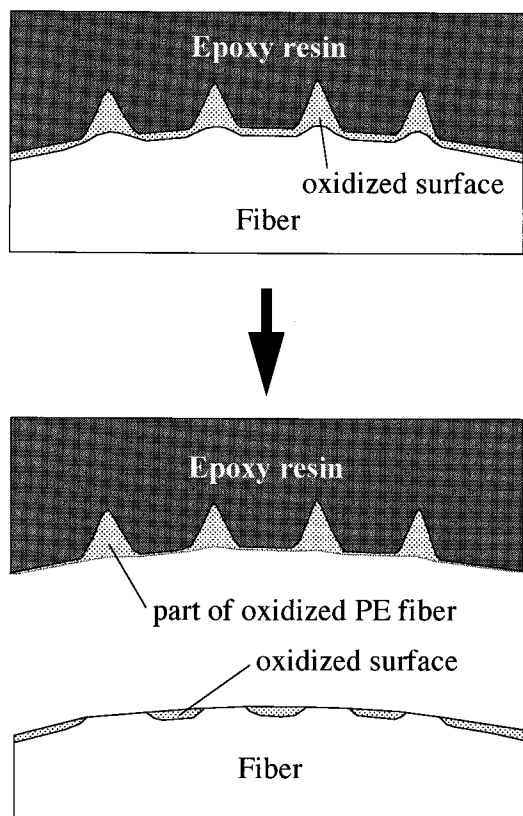


Figure 12 Schematic illustration of the sheared interface in the cross section for the PE/epoxy system in high-radiation energy.

%). In other words, this result reveals that complete adhesive failure did not occur in the shearing test.

To elucidate the fractured surfaces more concretely, the surfaces were observed with scanning electron microscopy. The results are shown in Figure 11. The peaked lines in the fiber direction on the surface of the PE fiber are very disturbed after the shearing test. Furthermore, some marks like a fine fiber can be observed on the surface of the epoxy-resin side after the shearing test. From these results, we can say that some peaked parts in the fiber were separated from the fiber surface and moved to the epoxy-resin side in the shearing test; thus, the fractured surfaces can be schematically shown (Fig. 12). This happened because the peaked parts in the fiber surface were completely oxidized and became weak in mechanical properties. In the shearing test, the peaked parts only moved to the epoxy-resin side and resulted in a lower oxygen content for the fractured surfaces than for the untreated fiber surface.

CONCLUSIONS

The tensile strength of the PE/epoxy composite reached 858 MPa with two corona treatments of the PE fiber, about 11 times greater than the value of the nontreated PE-fiber composite. The elastic modulus approached predicted values. However, the tensile strength was only 70% of the predicted strength. This was due to the molecular degradation of the PE-fiber surface caused by surface modification.

REFERENCES

1. Yamashita, A. *Shinsozai Jpn* 1993, 4, 38.
2. Porter, R. S.; Kanamoto, T. *Polym Eng Sci* 1994, 34, 266.
3. Werff, H.; Pennings, A. J. *Colloid Polym Sci* 1991, 269, 747.
4. Payer, W. *Kunstst Ger Plast* 1993, 83, 775.
5. Colvin, R. *Mod Plast Int* 1995, 25, 18.
6. Ogawa, T.; Mukai, H.; Osawa, S. *J Appl Polym Sci* 1998, 68, 1431.
7. Andreopoulos, A. G.; Tarantili, P. A. *J Elast Plast* 1998, 30, 118.
8. Strobel, J. M.; Strobel, M.; Lyons, C. S.; Dunatov, C.; Perron, S. J. *J Adhes Sci Technol* 1991, 5, 119.
9. Lee, J. H.; Kim, H. G.; Khang, G. S.; Lee, H. B.; Jhon, M. S. *J Colloid Interface Sci* 1992, 151, 563.
10. Lanauze, J. A.; Myers, D. L. *J Appl Polym Sci* 1990, 40, 595.
11. Vaykhansky, L. E.; Cohen, Y. *J Polym Sci Part B: Polym Phys* 1995, 33, 1031.
12. Mercx, F. P. M.; Benzina, A.; Langeveld, A. D. V.; Lemstra, P. J. *J Mater Sci* 1993, 28, 753.
13. Rarichandran, V.; Obendorf, S. K. *Polym Adv Technol* 1994, 5, 818.
14. Ladizesky, N. H.; Ward, I. M. *J Mater Sci* 1983, 18, 533.
15. Ladizesky, N. H.; Ward, I. M. *Compos Sci Technol* 1986, 26, 129.
16. Tissington, B.; Pollard, G.; Ward, I. M. *Compos Sci Technol* 1992, 44, 197.
17. Nguyen, H. X.; Weedon, G. C.; Chang, H. W. *Int SAMPE Symp* 1989, 34, 1603.
18. Bettge, D. J.; Hinrichsen, G. *Compos Sci Technol* 1993, 47, 131.
19. Li, Z.-F.; Grubb, T. *J Mater Sci* 1994, 29, 189.
20. Grubb, D. T.; Li, Z.-F. *J Mater Sci* 1994, 29, 203.
21. Peijs, T.; Rijdsdijk, H. A.; Kok, J. M. M.; Lemstra, P. J. *Compos Sci Technol* 1994, 52, 449.
22. Ogawa, T.; Mukai, H.; Osawa, S. *J Appl Polym Sci* 1999, 71, 243.
23. Tissington, B.; Pollard, G.; Ward, I. M. *J Mater Sci* 1991, 26, 82.
24. Ogawa, T.; Uchibori, H. *J Appl Polym Sci* 1994, 47, 245.